Staphylococcus aureus abscess communities and osteomyelitis

Host-pathogen interactions in vitro and in vivo
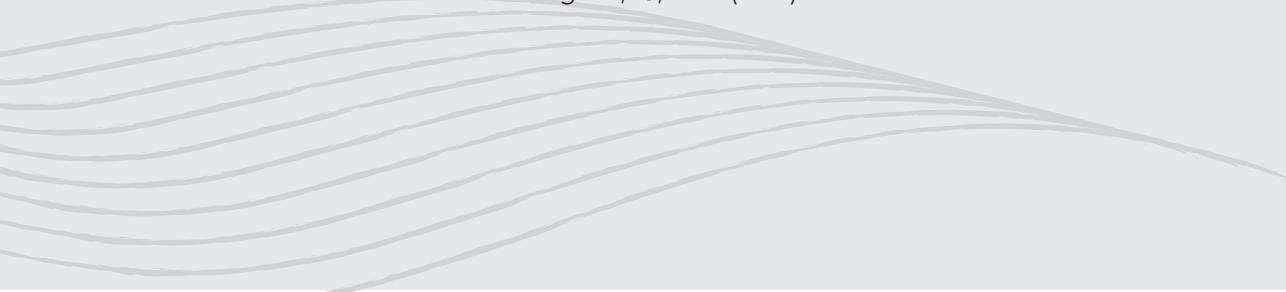
Hofstee, M.I.

Publication date
2022

CHAPTER 4

In vitro 3D *Staphylococcus aureus* abscess communities induce bone marrow cells to expand into myeloid-derived suppressor cells.

Marloes I. Hofstee, Anja Heider, Sonja Häckel, Caroline Constant, Martijn Riool, R. Geoff Richards, T. Fintan Moriarty, and Sebastian A. J. Zaat

ABSTRACT

Staphylococcus aureus is the main causative pathogen of subcutaneous, bone, and implant-related infections, forming structures known as staphylococcal abscess communities (SACs) within tissues that also contain immunosuppressive myeloid-derived suppressor cells (MDSCs). Although both SACs and MDSCs are present in chronic *S. aureus* infections, it remains unknown whether SACs directly trigger MDSC expansion.

To investigate this, a previously developed 3D *in vitro* SAC model was co-cultured with murine and human bone marrow cells. Subsequently, it was shown that SAC-exposed human CD11b$^{low/-}$ myeloid cells or SAC-exposed murine CD11b$^+$ Gr-1$^+$ cells were immunosuppressive mainly by reducing absolute CD4$^+$ and CD8α$^+$ T cell numbers as shown in T cell proliferation assays and with flow cytometry. Monocytic MDSCs from mice with an *S. aureus* bone infection also strongly reduced CD4$^+$ and CD8α$^+$ T cell numbers. With protein biomarker analysis and an immunoassay, we detected in SAC – bone marrow co-cultures high levels of GM-CSF, IL-6, VEGF, IL-1β, TNFα, IL-10, and TGF-β. Furthermore, SAC-exposed neutrophils expressed Arg-1 and SAC-exposed monocytes expressed Arg-1 and iNOS as shown with immunofluorescent stains.

Overall, this study showed that SACs cause MDSC expansion from bone marrow cells and identified possible mediators to target as additional strategy for treating chronic *S. aureus* infections.

INTRODUCTION

Staphylococcus aureus is an opportunistic pathogen that can cause a range of infections including subcutaneous, bone, and implant-related infections. A key common feature amongst these infections are biofilm and staphylococcal abscess communities (SACs)[1-4]. The outer margin of a typical abscess comprises collagen and fibrinogen that enclose a minority of monocytes and M2 macrophages and many neutrophils with the fibrin-encapsulated SAC at the center[3].

Myeloid-derived suppressor cells (MDSCs) are immature myeloid cells, either monocytic (M-MDSCs; CD11b^{+}, Ly6C^{high}, Ly6G^{−}) or granulocytic (G-MDSCs; CD11b^{+}, Ly6C^{low}, Ly6G^{+}), that suppress other immune cells such as T cells[5-7]. One way MDSCs suppress T cell proliferation is by depleting L-arginine from their surrounding milieu through upregulation of the enzymes arginase-1 (Arg-1) and inducible nitric oxide synthase (iNOS) that metabolize L-arginine, a metabolite important for the T-cell receptor (TCR) zeta chain and, thus, for T cell activation[7-9]. MDSC expansion has been observed in patients with cancer, inflammation, autoimmune diseases, and chronic infections, and have been linked to increased myelopoiesis after a decrease in myeloid cell numbers[10]. The growth factors granulocyte macrophage-colony stimulating factor (GM-CSF), granulocyte-colony stimulating factor (G-CSF), macrophage-colony stimulating factor (M-CSF), and vascular endothelial growth factor (VEGF), and the cytokine interleukin (IL)-6 are the main drivers of MDSC expansion by activation of the transcription factor STAT3[7,11,12]. During a bacterial infection, activation of MDSCs can either occur directly by toll-like receptor (TLR) ligands, such as *S. aureus* lipoproteins, or indirectly by prolonged exposure to pro-inflammatory cytokines such as IL-1β, TNFα, or IFNγ[12].

MDSCs were originally described in cancer patients approximately 30 years ago[10]. More recently, MDSCs have been identified in chronic *S. aureus* infections varying from subcutaneous infections[13] to implant-related biofilm/soft tissue infections[14-17]. Additionally, we have shown in our recent publication that MDSCs are also present in bone marrow of mice with an *S. aureus* osteomyelitis[3]. In that study, we showed that the neutrophils and monocytes around SACs and present within abscesses were alive, had an immature appearance, and had the typical phenotypical

4

MDSC-markers (CD11b^{+}, Ly6C^{high}, Ly6G^{−} or CD11b^{+}, Ly6C^{low}, Ly6G^{+})[3]. Moreover, immunosuppressive regulatory T cells (Tregs)[3,18] and anti-inflammatory, M2 macrophages[3,19] were observed surrounding the abscesses. These cells are commonly present in the MDSC-rich tumor microenvironment and are induced by MDSCs[10,20]. These previous studies, therefore, suggest that the cells around SACs and within the SAC-surrounding abscesses might be immunosuppressive MDSCs. However, it remains to be confirmed whether the SAC itself causes MDSCs to expand from bone marrow cells.

The aim of this study, therefore, was to examine whether SACs prime bone marrow cells to develop immunosuppressive abilities and to an MDSC phenotype by functional assays. Functional assays evaluate T cell function activity (*e.g.* T cell proliferation) and whether cells that potentially are MDSCs modulate this[8]. To enable studies into SAC formation, growth, and host cell interactions, a 3D *in vitro* SAC model was previously developed in our lab[21]. These *in vitro* SACs are encased with a fibrin layer and are not penetrated by neutrophils, as also observed for *in vivo* SACs, and they were resistant to high doses of the antibiotics gentamicin and rifampicin[21]. In this study, we investigated the interaction of the *in vitro* SAC model with both murine and human bone marrow cells to determine their immunosuppressive activity and the secreted proteins.

MATERIALS AND METHODS

Bacteria

Clinical isolate *S. aureus* JAR 06.01.31 (the culture collection of Switzerland (CCOS) number 890, Wädenswill, Switzerland), obtained from a patient with an orthopaedic device-related infection[22], was used in this study. *S. epidermidis* O-47, originally isolated from a patient at the Institute Für Medizinische Mikrobiologie und Hygiene, University of Cologne (Germany)[23], was used as a coagulase-negative strain.

In vitro SAC model

In vitro SACs were produced as described previously[21] with some minor adjustments. Briefly, 10 µl collagen gel was prepared from rat collagen

type I solution (1.78 mg/ml, pH 7.4; Gibco, Basel, Switzerland) following manufacturer's instructions, and was added to a 24-well Transwell system (polyester membrane with a porosity of 0.4 µm; Corning Life Sciences B.V., Amsterdam, the Netherlands) and let to polymerize for 1 h at 37 °C in a humidified incubator. After 1 h, a 25 µl bacterial solution containing approximately 14 colony forming units (CFUs) of *S. aureus* JAR 06.01.31 was pipetted on top of the collagen gel together with 75 µl homogenized collagen and 300 µl pooled human plasma (Regional Blood Donation Service SRK Graubünden, Chur, Switzerland). Samples were incubated overnight at 37 °C and an additional 300 µl pooled human plasma was supplied after 5 h of incubation (Figure 1A).

In addition to *S. aureus*, the same procedure was applied to *S. epidermidis* O-47, resulting in small aggregates of the bacterium within gel. As an additional control, approximately 2.5×10^5 log-phase *S. aureus* JAR 06.01.31 were added to 100 µl collagen gel and mixed to obtain a dispersed bacterial presence throughout the gel, but no concentrated, fibrin encased SAC.

Murine bone marrow cell and splenocyte isolation

After washing the femoral and tibial bones in Hanks' buffered salt solution (HBSS; Gibco) and removing the outer ends of the bones, the bone marrow cells were flushed out with a 26G × 1" needle attached to a 2 ml syringe (both Braunn, Davos Platz, Switzerland) containing HBSS. The collected cells were passed through a 70 µm cell strainer, centrifuged at 300 × g for 6 min at 4 °C, supernatant was removed, and the cell pellet was incubated in 5 ml erythrocyte lysis buffer (15 mM NH_4Cl, 1 µM $KHCO_3$ and 10 µM disodium ethylenediaminetetraacetic acid; all Sigma-Aldrich, Buchs, Switzerland) for 5 min at RT. Subsequently, 25 ml Roswell Park Memorial Institute 1640 (RPMI; Gibco) supplemented with 3 % fetal bovine serum (FBS; Sigma-Aldrich) was added to neutralize the lysis buffer. The washed and isolated cells were centrifuged at 300 × g for 6 min at 4 °C, resuspended in freezing medium consisting of RPMI with 40 % FBS and 10 % dimethyl sulfoxide (DMSO; Sigma-Aldrich), and stored in liquid nitrogen until further use.

Spleens were pushed through a 70 µm cell strainer that was placed on a 50 ml tube with the plunger of a 5 ml syringe to isolate splenocytes. The cell

4

strainer was washed with 5 ml RPMI with 3 % FBS, the cell suspension was centrifuged at 300 × g for 6 min at 4 °C, supernatant was discarded, and lysis buffer was applied for 4 min at RT. After adding 25 ml RPMI with 3 % FBS, cells were spun down at 300 × g for 6 min at 4 °C, washed with 10 ml RPMI with 10 % FBS, centrifuged at 300 × g for 6 min at 4 °C, and resuspended in 20 ml RPMI with 10 % FBS. The splenocyte suspension was filtered with a 40 µm cell strainer, resuspended in freezing medium, and stored in liquid nitrogen until further use.

In vitro SAC – murine bone marrow co-cultures

After overnight culture, two *in vitro* SAC samples were removed from the 24-well Transwell and placed into a 6 well plate. Murine bone marrow cells (1 × 10^6 per well) were cultured in RPMI with 10 % FBS, 1 mM sodium pyruvate (Sigma-Aldrich), and 50 µM β-mercaptoethanol (Roth AG, Arlesheim, Switzerland) and either did not receive any further supplements (negative control), were supplemented with 40 ng/ml IL-6 and GM-CSF (positive control; both Peprotech, London, United Kingdom), or exposed to *in vitro* SACs and all three conditions were cultured for 3 d at 37 °C with 5 % CO_2. Thereafter, *in vitro* SACs were removed from the wells and discarded, and the bone marrow cells from the three different conditions were collected on ice by using a cell scraper. Approximately 50,000 cells were kept aside, stained for CD11b-APC, Ly6G-FITC, Ly6C-PE (all Biolegend, Fell, Germany), and DAPI (Sigma-Aldrich) and analysed with the flow cytometer BD FACSDiva (BD Bioscience, Allschwil, Switzerland). From the remaining bone marrow cells, $CD11b^+$ Gr^+ cells were purified by using the EasySep™ Mouse MDSC (CD11b+Gr-1+) isolation kit (StemCell, Saint Egrève, France) following the manufacturer's protocol.

For the co-cultures with *S. epidermidis* aggregates or *S. aureus* in gel, 2.5 × 10^5 murine bone marrow cells were added in RPMI supplemented with 10 % FBS, 1 mM sodium pyruvate, and 50 µM β-mercaptoethanol to a 24 wells plate and cultured for 3 d at 37 °C with 5 % CO_2. Then, the *S. epidermidis* aggregates or *S. aureus* in gel were removed from the samples, the bone marrow cells were collected on ice by using a cell scraper, stained for CD11b-APC, Ly6G-FITC, Ly6C-PE, and DAPI and acquired with the flow cytometer BD FACSDiva.

Murine T cell proliferation assay

Splenocytes were stained with the membrane dye PKH26 (Sigma-Aldrich) using manufacturer's instructions. For the T cell proliferation assay, the PKH26-stained splenocytes were plated at 2.5×10^4/well of a 96-wells plate in RPMI supplemented with 10 % FBS, 1 % (v/v) penicillin/streptomycin solution (Gibco), 1 mM sodium pyruvate, and 50 µM β-mercaptoethanol. Splenocytes were either unstimulated and cultured as a monoculture or splenocytes were stimulated with murine CD3/CD28 Dynabeads (Thermofisher Scientific, Darmstadt, Germany; 1:1 ratio) and 30 U/ml murine rIL-2 (Peprotech) and cultured as a monoculture or as a co-culture with purified $CD11b^+$ Gr^+ bone marrow cells in a 1:1 or 1:0.5 cell ratio. The cells were incubated for 3 d at 37 °C with 5 % CO_2 and, subsequently, T cells were assessed for their proliferation rate and cell numbers by flow cytometry. Cells were stained for CD3-FITC, CD4-Alexa Fluor 700, CD8α-APC antibodies (all Biolegend), and DAPI, and collected in TruCount tubes (BD Bioscience). Proliferation was normalized to T cells stimulated with CD3/CD28 Dynabeads and rIL-2, which were set to 100 %.

4

Human bone marrow cell and PBMC isolation

$CD33^+$ myeloid cells were enriched from human bone marrow aspirates of four different donors by using the RosetteSep™ HLA myeloid cell enrichment kit (StemCell). In short, bone marrow aspirates were incubated with RosetteSep™ HLA cocktail for 20 min at RT, diluted 1:1 with HBSS with 2 % FBS, layered on top of 10 ml RosetteSep™ DM-M Density Medium, and centrifuged at $330 \times g$ for 25 min without brakes. The enriched cells were removed, and remaining erythrocytes were lysed using 5 ml lysis buffer as mentioned above.

PBMCs were isolated from EDTA-whole blood and density-gradient centrifugation with Lymphoprep (StemCell) as density gradient medium following the manufacturer's protocol.

In vitro SAC – human bone marrow co-cultures

Myeloid enriched bone marrow cells were cultured 2×10^6 per well of 6 wells plate in Iscove's Modified Dulbecco's Medium (IMDM; Avantor, Dietikon,

Switzerland) supplemented with 10 % FBS, 0.01 M HEPES (Thermofisher Scientific), 0.55 mM arginine (Sigma-Aldrich), 0.24 mM asparagine (Sigma-Aldrich), 1.5 mM glutamine (Sigma-Aldrich), and 50 µM β-mercaptoethanol for 3 d at 37 °C with 5 % CO_2[24]. A part of the cells were also exposed to overnight grown *in vitro* SACs or were supplemented with 40 ng/ml GM-CSF and G-CSF (Peprotech) and cultured with 8 % CO_2[24]. Cells were harvested as mentioned above and CD11b^{low/−} cells were isolated with the EasySep™ "Do-It-Yourself" positive selection kit using an anti-human CD11b antibody (both StemCell) as selection antibody. The kit was used as described by the manufacturer, but instead of collecting the isolated CD11b^{+} cells the remaining CD11b^{low/−} cells were collected.

Human T cell proliferation assay

The CD11b^{low/−} cells were co-cultured with 2.5×10^4 PKH26-stained PBMCs in a 1:1 ratio in RPMI 1640 medium for SILAC (Thermofisher Scientific) with 150 µM arginine, 218.5 µM L-lysine monohydrochloride (Sigma-Aldrich), human CD3/CD28 Dynabeads (Thermofisher Scientific; 1:1 ratio), and 30 U/ml human rIL-2 (Peprotech) for 4 d at 37 °C with 5 % CO_2. PBMCs were also cultured either unstimulated or stimulated with human CD3/CD28 Dynabeads and 30 U/ml human rIL-2. Cells were collected, stained for CD3-BV605, CD4-FITC, CD8α-APC antibodies (all Biolegend), and DAPI, and transferred to TruCount tubes, and T cells numbers were assessed with flow analysis. The number of T cells from the stimulated PBMC monocultures were set to a 100 % and used for normalization of the other samples with.

In vivo samples

Ex vivo cell culture supernatant from splenocytes co-cultured with either FACS sorted CD11b^{+} Ly6C^{+} Ly6G^{−} or CD11b^{+} Ly6C^{+} Ly6G^{+} bone marrow cells from infected or non-infected mice were obtained from a study approved by the ethical committee of the canton of Graubünden in Switzerland (approval number 2019_10) and previously reported[3]. In short, specific pathogen-free (SPF) C57Bl/6N female mice (Charles River, Sulzland, Germany) of 20 to 28 weeks old received as surgical intervention a double osteotomy of the left femur after the bone was stabilized with a titanium 6-hole MouseFix locking

plate (RISystems AG, Davos Platz, Switzerland) by inserting the 4-outermost screws. The 2 mm segment created was taken out and inoculated with 1 µl PBS containing approximately 1×10^4 CFU of *S. aureus* JAR 06.01.31 or 1 µl sterile PBS. The inoculum or saline was allowed to absorb into the bone for 3 min and the segment was placed back into its original place without fixation. The fascia lata and the skin are closed with continuous sutures (5-0 Vicryl rapide, Ethicon, Courcelles, Belgium). At 21 days post-operative, animals were sacrificed, and bone marrow for the left femurs was isolation as mentioned above. Monocytes (CD11b$^+$ Ly6C$^+$ Ly6G$^-$) or neutrophils (CD11b$^+$ Ly6C$^+$ Ly6G$^+$) from the isolated bone marrow were sorted with a BD FACSDiva (BD Bioscience) by using the anti-CD11b-APC, anti Ly6G-FITC, and anti Ly6C-PE (all Biolegend) and DAPI. Cells were sorted with an efficiency above 86 % and purified cells were kept on ice until further use. With the FACS-sorted monocytes or neutrophils a murine T cell proliferation assay was performed.

Immunofluorescent and histochemical stains

For immunofluorescent stains, fixed samples were first blocked with 1:20 diluted animal-free blocker (Vector Laboratories, Burlingame, CA, USA) in PBS with 1 % Triton X (PBS-T; Sigma-Aldrich) for 1 h at RT. Blocking buffer was removed, primary antibodies (Table 1) diluted 1:200 were added to the samples and incubated for 1 h at RT. Subsequently, samples were washed 3 times with PBS-T for 5 min, if applicable, secondary antibodies (1:200 dilution; Table 1) were added to the samples and incubated for 30 min in the dark at RT. Lastly, samples were washed 3 times with PBS-T for 5 min and a PBS solution with DAPI was added.

Haematoxylin & eosin stains were done with Mayer's hematoxylin and a 0.25 % eosin solution (both Sigma-Aldrich).

Protein biomarker analysis

In vitro cell culture supernatants of murine bone marrow cells (negative control, positive control, or co-cultures with *in vitro* SAC) and *ex vivo* cell culture supernatant from splenocytes co-cultured with either FACS sorted CD11b$^+$ Ly6C$^+$ Ly6G$^-$ or CD11b$^+$ Ly6C$^+$ Ly6G$^+$ bone marrow cells from infected or non-infected mice were analysed with the mouse exploratory panel (Olink,

4

Uppsala, Sweden) using manufacturer's instructions. Data are shown as normalized protein expression values, which is an arbitrary unit in a Log2 scale of Olink and are calculated from Ct values.

Table 1, A list with all primary antibodies used and their accompanying secondary antibodies.

Primary antibody	Dilution	Secondary antibody
Rat monoclonal anti-Ly6G antibody (BD Bioscience, 551459) conjugated with Alexa Fluor® 647 (Abcam, ab269823)	1:50	-
Rat monoclonal anti-Ly-6C antibody (Biolegend, 128002) conjugated with Alexa Fluor® 488 (Abcam, ab236553)	1:25	-
Rat monoclonal anti-Ly6G antibody	1:50	Goat anti-rat IgG Alexa Fluor 488
Rat monoclonal anti-Ly-6C antibody	1:25	Goat anti-rat IgG Alexa Fluor 488
Rabbit polyclonal anti-iNOS antibody (Abcam, ab15323)	1:50	Goat anti-rabbit IgG Alexa Fluor 568
Goat polyclonal anti-arginase 1 antibody (Genetex, GTX88484)	1:200	Donkey anti-goat IgG Alexa Fluor Plus 647

Cytokine and growth factor measurements

In vitro cell culture supernatants of human bone marrow cells (negative control, positive control, or co-cultures with *in vitro* SAC) were assessed on GM-CSF, IFN-γ, IL-6, TNFα, IL-1β, IL-12p70, IL-8, and IL-10 presence by using a U-plex, multiplex assays (MSD, Rockville, MD, United States).

Data analysis

Flow cytometric data was analysed with Kaluza Analysis Software (Beckman Coulter Life Sciences, Indianapolis, IN, USA). Statistical analysis of the Olink data was performed used the online Olink Insights Stat Analysis tool (Olink) by using an ANOVA with Tukey's post hoc test as statistical test, and Olink data visualization was done with GraphPad Prism 8 (GraphPad Software, San Diego, CA, United States). Statistical analysis of the flow cytometry data was performed with GraphPad Prism 8. Normality of data was checked with a Shapiro-Wilk test and, subsequently, analysed with a Holm-Sidak's

or Tukey's multiple comparison test. *p*-values of <0.05 were considered statistically significant.

RESULTS

Murine bone marrow cells co-cultured with S. aureus SACs

The *in vitro* SAC model was co-cultured with murine bone marrow cells (Figure 1A) to explore whether bacteria within a SAC can elicit bone marrow cells to adopt an MDSC phenotype. Murine bone marrow cells were either left untreated as a negative control (no MDSC expansion) or supplemented with IL-6 and GM-CSF as a positive control for MDSC expansion. Furthermore, murine bone marrow cells were co-cultured either with *S. aureus* dispersed in a collagen gel or *S. epidermidis* aggregates, to determine whether observed effects were SAC specific. The percentages of monocytes and neutrophils from alive CD11b$^+$ cells were determined with flow cytometry for the above-mentioned samples as these might change when cells expand into MDSCs (Figure 1B and C). Compared to the negative control, the positive control and the SAC-exposed bone marrow cultures contained significantly more Ly6C$^+$ monocytes (p < 0.0001 and p = 0.0028, respectively). However, the percentage of monocytes in SAC-exposed co-cultures was less than for the positive control (p = 0.0003) and did not differ from the numbers in the co-cultures with dispersed *S. aureus*. Co-cultures with *S. epidermidis* aggregates had a small percentage of monocytes present. Percentages of Ly6G$^+$ neutrophils of the negative control were significantly higher than in the positive control and SAC-exposed cultures (p < 0.0001 and p < 0.0001, respectively), which contained similar neutrophil percentages. The percentage of neutrophils in bone marrow – SAC co-cultures was also significantly lower than in the co-cultures with dispersed *S. aureus* and with *S. epidermidis* aggregates (p = 0.0001 and p < 0.0001, respectively).

Next, the morphological appearance and a Ly6C (monocytes) and Ly6G (neutrophils) double-staining of the cells from the different conditions were examined (Figure 1D). The negative control bone marrow cells were mainly small, Ly6G$^+$ cells. In contrast, the positive control bone marrow cells had clusters of elongated, Ly6C$^+$ cells with some smaller, Ly6G$^+$ cells. Similar cells

4
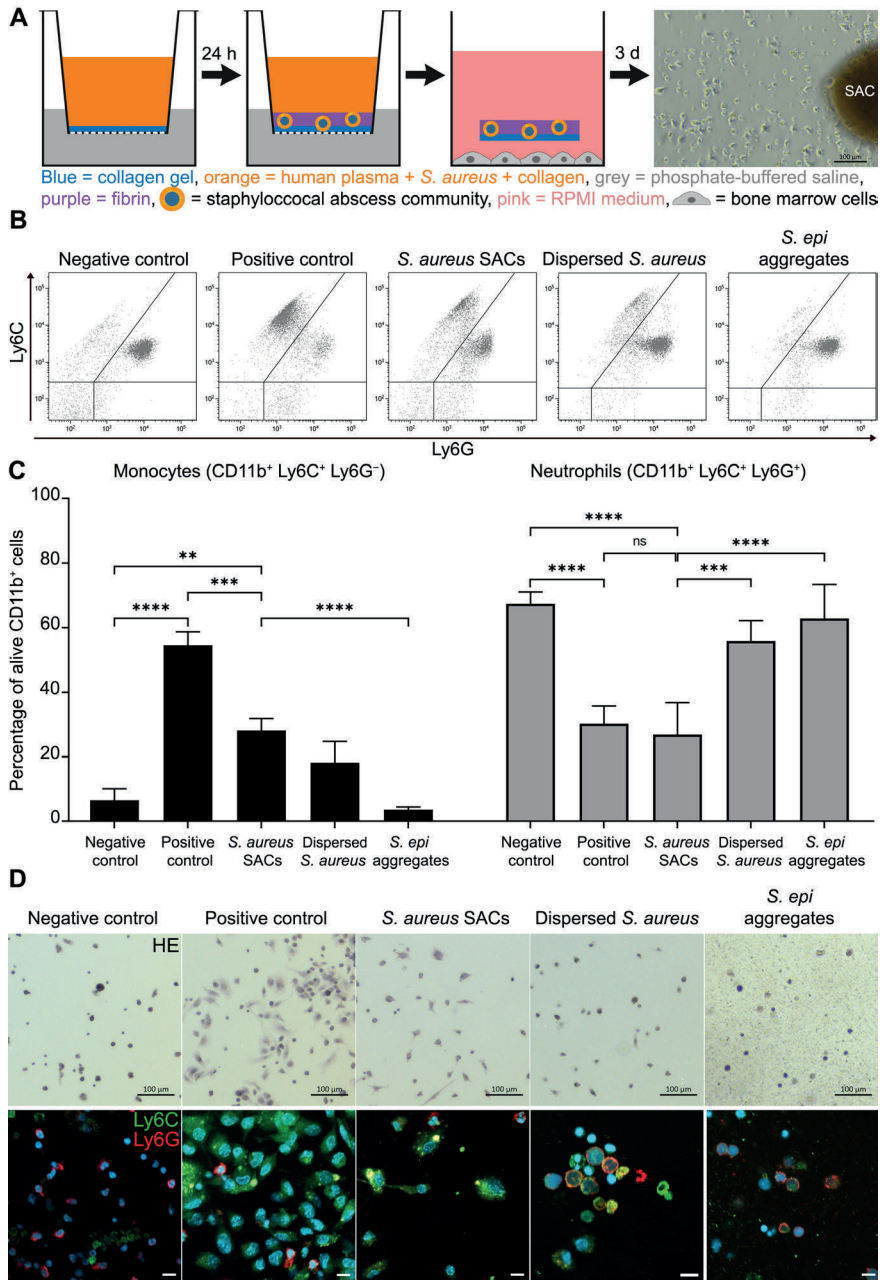
Figure 1, Murine bone marrow cells were co-cultured with *in vitro S. aureus* SACs.
(A) A schematic overview of how the *in vitro* SACs were generated and how the bone
marrow cells were co-cultured with *in vitro* SACs. As comparison to this co-culture,
murine bone marrow cells were kept untreated (negative control), were treated with

GM-CSF and IL-6 (positive control), or were co-cultured with dispersed *S. aureus* in a collagen gel or *S. epidermidis* aggregates. The percentage of monocytes (Ly6C$^+$) and neutrophils (Ly6G$^+$) from alive CD11b$^+$ cells was determined with flow analysis and are depicted as (B) flow pots or (C) bar graphs. Data are mean (±SD) and are from three independent experiments with three replicates per test. (D) Negative control, positive control, *S. aureus* SAC, dispersed *S. aureus*, or *S. epidermidis* aggregates-exposed murine bone marrow cells were stained with haematoxylin and eosin (upper row) or with antibodies (lower row) for Ly6C (green; monocytes) and Ly6G (red; neutrophils) combined with DAPI as nuclear stain (blue). Scale bar = 10 µm. Statistical test used: Tukey's multiple comparison test. ns = non-significant, **p < 0.01, ***p < 0.001, and ****p < 0.0001.

were observed in the bone marrow – SAC co-culture. Bone marrow cells exposed to dispersed *S. aureus* also contained a few elongated, Ly6C$^+$ cells but had mostly round, Ly6G$^+$ cells present. The bone marrow cells co-cultured with *S. epidermidis* aggregates were round, Ly6G$^+$ cells.

T cell proliferation with S. aureus SAC-exposed murine CD11b$^+$ Gr$^+$ bone marrow cells

To test whether SAC-exposed bone marrow monocytes and neutrophils have immunosuppressive abilities, bone marrow cells positive for CD11b and Gr-1 (an antibody against both Ly6C and Ly6G, hence for both monocytes and neutrophils) were isolated. Furthermore, the isolated cells were used in a T cell proliferation assay where PKH26-stained splenocytes (mostly T cells) receive an anti-CD3/28 stimulus to induce T cell activation and expansion. Next, proliferation rates and absolute cell numbers of the two major T cell subtypes CD4$^+$ T helper cells and cytotoxic, CD8α$^+$ T cells were quantified as these should decrease in the presence of immunosuppressive cells (Figure 2). Compared to the negative control, CD11b$^+$ Gr-1$^+$ bone marrow cells from the positive control when cultured in a 1:1 or 0.5:1 ratio with splenocytes significantly reduced the percentage of proliferated CD4$^+$ T cells (p < 0.0001 and p = 0.0012, respectively; Figure 2A) as well as the absolute CD4$^+$ T cells numbers (p < 0.0001 and p = 0.0014, respectively; Figure 2B). SAC-exposed CD11b$^+$ Gr-1$^+$ bone marrow cells co-cultured in a 1:1 ratio with splenocytes also significantly reduced the percentage of proliferated CD4$^+$ T cells (p = 0.036; Figure 2A) and the absolute CD4$^+$ T cells numbers (p = 0.0022; Figure 2B) compared to the negative control, although to a lesser extent than the positive control. These effects were less pronounced in the 0.5:1 ratio culture

4

with splenocytes (p = 0.37 and p = 0.046, respectively). In comparison to the negative control, the positive control CD11b+ Gr-1+ bone marrow cells significantly decreased the CD8α+ T cell proliferation rates. This was true for both the 1:1 and 0.5:1 ratio cultures (p < 0.0001 and p = 0.0057, respectively; Figure 2C). Furthermore, positive control bone marrow cells significantly decreased absolute CD8α+ T cell numbers in both the 1:1 and 0.5:1 ratio cultures (p < 0.0001 and p = 0.0026, respectively; Figure 2D) compared to the negative control. However, the SAC-exposed CD11b+ Gr-1+ bone marrow cells had 15.6 % lower absolute CD8α+ T cell numbers than the negative control
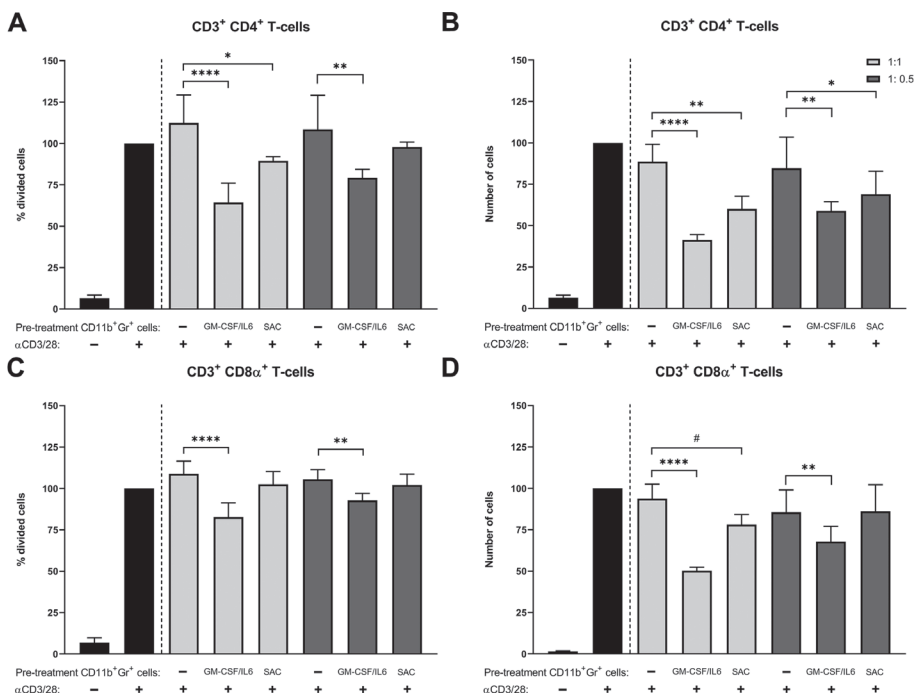

Figure 2, T cell proliferation assays with negative control, positive control or *S. aureus* SAC-exposed murine monocytes and neutrophils. (A) Proliferation rates and (B) absolute cell numbers of CD3+ CD4+ T cells and (C) proliferation rates and (D) absolute cell numbers of CD3+ CD8α+ T cells were determined with flow analysis of PKH-stained splenocytes mono-cultures (black) without or with anti-CD3/CD28 stimulation and from PKH-stained and anti-CD3/CD28-stimulated splenocytes co-cultured with CD11b+ Gr-1+ monocytes and neutrophils from negative control, positive control, or *S. aureus* SAC co-culture samples in a 1:1 ratio (light grey) or 1:0.5 ratio (dark grey). Data are mean (±SD) and are from four independent experiments with three replicates per test. Statistical test used: Holm-Sidak's multiple comparison test. #p ≤ 0.1, *p < 0.05, **p < 0.01, and ****p < 0.0001.

(p = 0.10; Figure 2D). These results showed that the positive control CD11b^{+} Gr-1^{+} bone marrow cells indeed had immunosuppressive abilities towards both CD4^{+} T cells and CD8α^{+} T cells and so were deemed to be MDSCs. Given that the SAC co-cultured CD11b^{+} Gr-1^{+} bone marrow cells had significant immunosuppressive activity towards CD4^{+} T cells, the SAC-exposed CD11b^{+} Gr-1^{+} bone marrow cells therefore can also be deemed to be MDSCs.

Expression of the MDSC-related enzymes iNOS and Arg-1 of S. aureus SAC-exposed murine bone marrow cells

To explore whether the immunosuppressive abilities of SAC-exposed CD11b^{+} Gr-1^{+} bone marrow cells are possibly facilitated by the enzymes iNOS and/or Arg-1, immunofluorescent stains for iNOS and Arg-1 were performed.
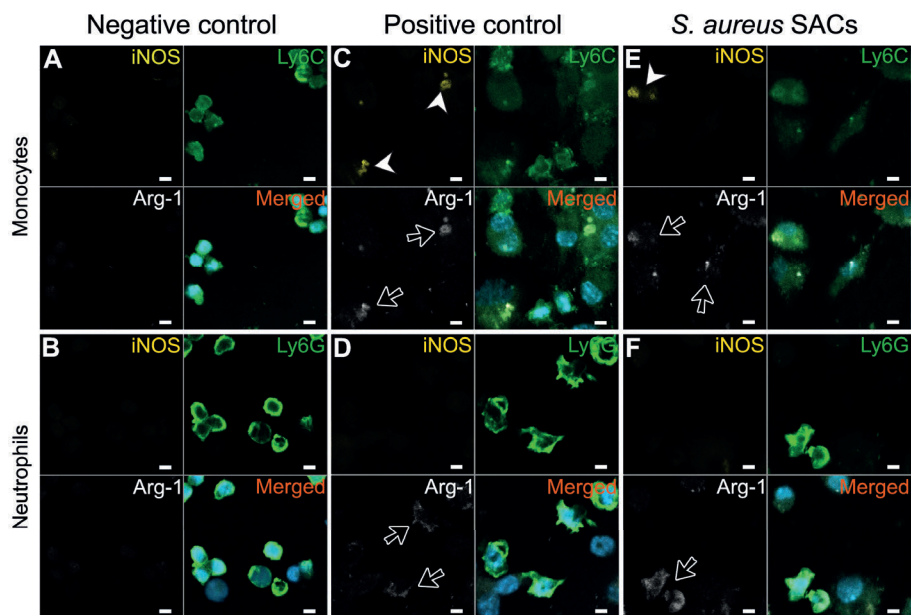
Figure 3, Representative immunofluorescent stains of monocytes or neutrophils for the MDSC-related enzymes iNOS and Arg-1. Untreated, negative control (A) monocytes or (B) neutrophils, GM-CSF and IL-6 treated, positive control (C) monocytes or (D) neutrophils, or *S. aureus* SAC-exposed (E) monocytes or (F) neutrophils (green) were stained for iNOS (yellow; white arrowhead) and Arg-1 (white; black arrow) with DAPI as nuclear stain (blue). Scale bar = 5 µm.

The monocytes and neutrophils from the negative control did not express iNOS and Arg-1 (Figure 3A and B, respectively). M-MDSCs from the positive control showed co-localization of the iNOS and Arg-1 stains at some spots (Figure 3C) and G-MDSCs from the positive control expressed Arg-1 (Figure 3D). Similar iNOS and Arg-1 expression patters were observed for the SAC-exposed murine bone marrow cells; the M-MDSCs were stained with both iNOS and Arg-1, and the G-MDSCs were only stained with Arg-1 (Figure 3E and F, respectively).

Secreted proteins by the murine bone marrow cells when exposed to in vitro SACs

The secreted proteins from SAC-exposed murine bone marrow cells after 3 d culture were analysed to possibly clarify which molecules might play a role in the immunosuppressive capabilities of these cells. The expression levels of a selection of secreted proteins indicative for various biological processes including immune responses, chemotaxis, and cell proliferation from SAC-exposed and positive control bone marrow cells were compared to the negative control (Table S1, containing all data). In total there were 53 proteins significantly differently expressed as compared to the negative control, of which 34 were unique for SAC – bone marrow co-cultures, 6 were unique for positive control cultures, and 13 were shared for both SAC-exposed bone marrow and positive control cultures (Figure 4A). Proteins that were higher expressed in positive control bone marrow cultures than the negative control were the enzymes RIOX1 and LPL, a modulator of lipid metabolism being PLIN1, and the cytokine TGF-α, whereas the enzymes PRDX5 and PARP1 were lower expressed (Figure 4B, upper part). Proteins that were solely secreted at a significantly higher level in SAC – bone marrow co-cultures and were potentially MDSC-related were chemoattractants (for neutrophils, monocytes, Tregs, and Th17 cells), cytokines such as IL-10 and TGF-β, apoptosis/cell survival mediators, growth factors including VEGF, and proteins of the Notch3, arginase/NO, glycolysis, or NF-κB signalling pathways (Figure 4B, lower part). Proteins secreted at a significantly higher level in both SAC – bone marrow and positive control cultures were chemokines (for neutrophils and monocytes), the growth factor GM-CSF, cytokines being IL-6, IL-1β, and TNFα, apoptosis/cell survival mediators, membrane proteins, the

proangiogenic proteins follistatin (FST), and the cysteine protease legumain (LGMN) (Figure 4C).
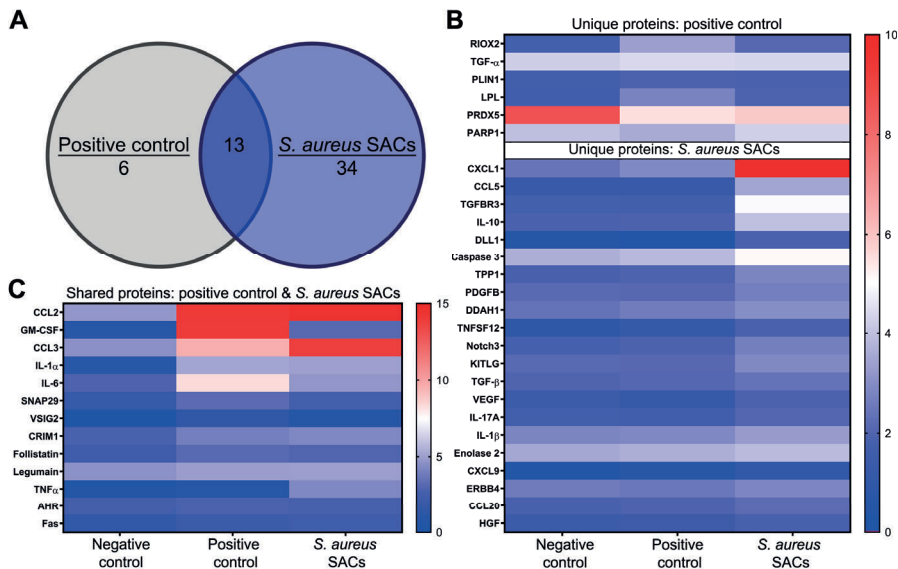
Figure 4, Protein biomarker analysis of supernatants from negative control, positive control, and *S. aureus* SAC-exposed murine bone marrow samples after 3 d culture. (A) Venn diagram highlighting the number of unique and shared significant proteins of positive control and SAC – bone marrow cultures in comparison to the negative control. Expression levels of (B) proteins that were significantly different in the positive control (upper part) or proteins of interest in the SAC – bone marrow cultures (lower part) compared to the negative control (0-5 = blue and 5-10 = red), and expression levels of (C) significant proteins in both the positive control and SAC – bone marrow cultures (0-7.5 = blue and 7.5-15 = red). Data are medians of normalized protein expression (NPX) values from three independent experiments, *n* = 9 per condition. Statistical test used: an ANOVA with a Tukey's post hoc tests.

T cell proliferation assays with monocytes or neutrophils from non-infected or S. aureus-infected mice

Monocytes or neutrophils isolated from bone marrow of non-infected mice or *S. aureus*-infected mice from a fracture fixation model were used in a T cell proliferation assay with PKH26-stained splenocytes to assess their effects on absolute CD4$^+$ and CD8α$^+$ T cell numbers. Compared to monocytes of non-infected mice, splenocyte co-cultures with monocytes from *S. aureus*-infected mice in a 0.5:1 and 1:1 ratio had significant lower numbers of CD4$^+$ T

cells (p = 0.020 and p = 0.0092, respectively; Figure 5A) and lower in numbers of CD8α⁺ T cell when co-cultured in a 1:1 ratio (p = 0.043; Figure 5B). Neither neutrophils from the *S. aureus*-infected mice or from the non-infected mice gave a difference in absolute T cell numbers. Co-cultures containing splenocytes and monocytes from *S. aureus*-infected mice and after a 4 d incubation had significantly more IL-17A, IL-17F, transforming growth factor beta (TGF-β), hepatocyte growth factor (HGF), and platelet-derived growth factor-B (PDGFB) and significantly less IL-10 compared to co-cultures of splenocytes and monocytes from non-infected mice (Figure 5C).
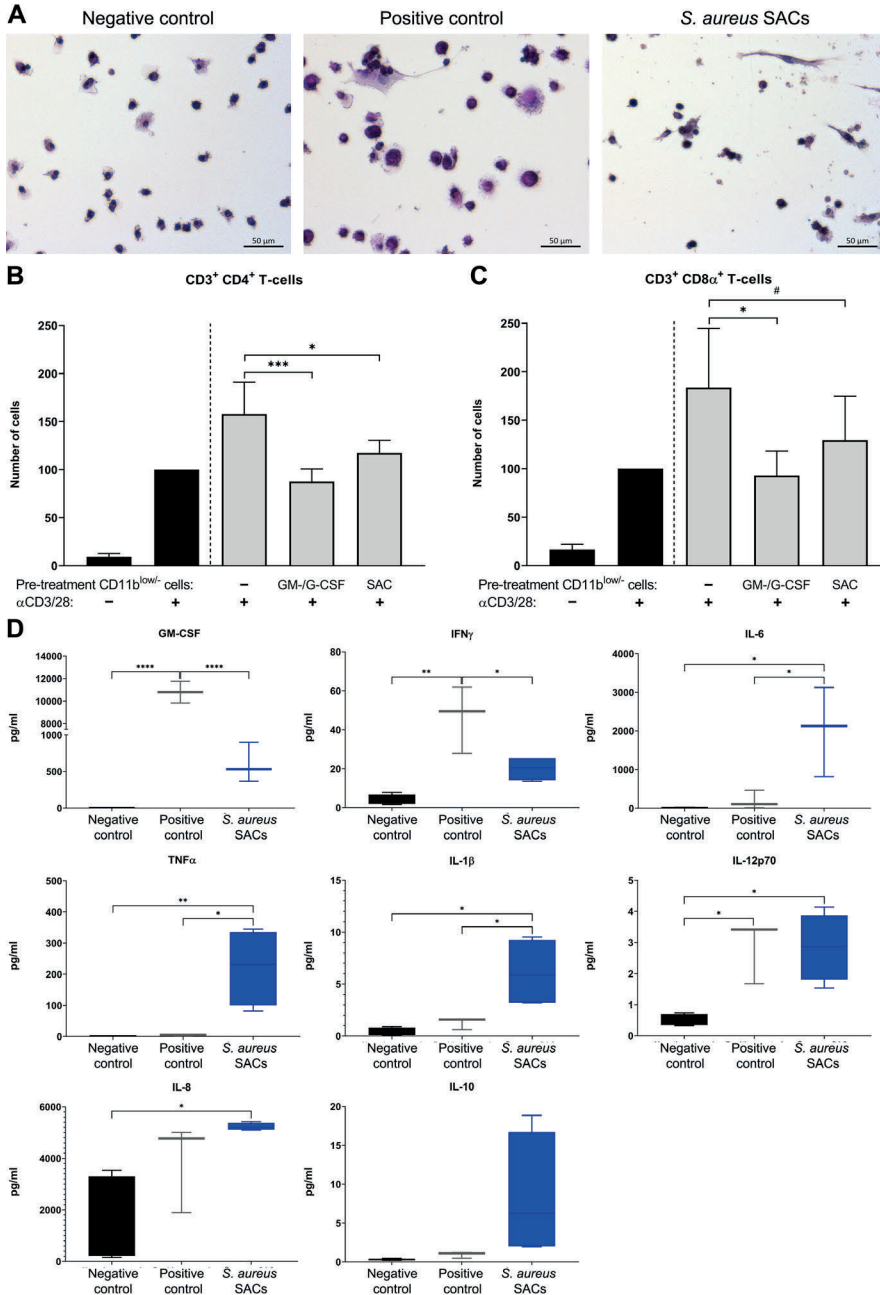
Human bone marrow cells co-cultured with S. aureus SACs

CD33⁺ myeloid cells, which include monocytes and neutrophils, obtained from human bone marrow were co-cultured with *in vitro* SACs to examine whether human bone marrow cells develop an MDSC phenotype. CD33⁺ myeloid cells from human bone marrow were left untreated as negative control or were treated with GM-CSF and G-CSF with 8 % CO_2 as positive control. In the preparations of the negative control only separate single cells with a round shape were observed, whereas in the positive control and SAC-exposed bone marrow cell preparations, in addition to clusters of cells, also contained cells with an elongated appearance (Figure 6A).

Subsequently, CD11b$^{low/-}$ myeloid cells, previously indicated to have the potential of becoming MDSCs[24-26], were isolated and used in a T cell proliferation assay with PKH26-stained human peripheral blood mononuclear cell (PBMCs; as a source of T cells) to assess their immunosuppressive abilities. Compared to CD11b$^{low/-}$ myeloid cells from negative control samples, positive control and SAC-exposed CD11b$^{low/-}$ myeloid cells significantly lowered the number of CD4⁺ T cell (p = 0.0002 and p = 0.010, respectively; Figure 6B). Furthermore, positive control CD11b$^{low/-}$ myeloid cells significantly lowered CD8α⁺ T cell numbers compared to the negative control (p = 0.011; Figure 6B), whereas SAC-exposed CD11b$^{low/-}$ myeloid cells lowered CD8α⁺ T cell numbers by 54.3 % (p = 0.10; Figure 6C).
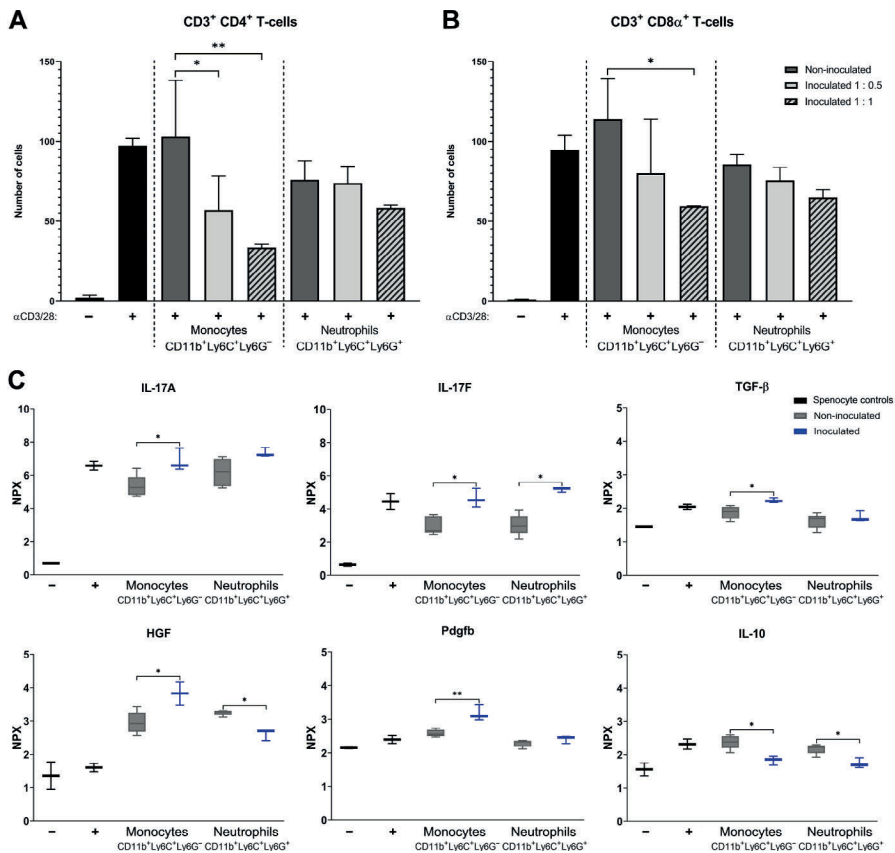
Figure 5, T cell proliferation assays with murine monocytes or neutrophils from non-inoculated or *S. aureus*-inoculated mice. (A) Absolute cell numbers of CD3^{+} CD4^{+} T cells and (B) absolute cell numbers of CD3^{+} CD8α^{+} T cells were determined with flow analysis of PKH-stained splenocytes mono-cultures (black) without or with anti-CD3/CD28 stimulation and from PKH-stained and anti-CD3/CD28-stimulated splenocytes co-cultured with CD11b^{+} Ly6C^{+} Ly6G^{-} monocytes or CD11b^{+} Ly6C^{+} Ly6G^{+} neutrophils from non-inoculated mice (1:1 ratio; dark-grey) or *S. aureus*-inoculated mice (1:0.5 ratio; light grey or 1:1 ratio; striped light grey). Results on T cell proliferation rates of these cultures were published previously[3]. Data are mean (±SD) and *n* = 5. Statistical test used: Holm-Sidak's multiple comparison test. (C) Normalized protein expression (NPX) values of proteins measured in supernatants of 4 d incubated PKH-stained splenocytes mono-cultures (black) without or with anti-CD3/CD28 stimulation and of PKH-stained and anti-CD3/CD28-stimulated splenocytes co-cultured 1:1 with CD11b^{+} Ly6C^{+} Ly6G^{-} monocytes or CD11b^{+} Ly6C^{+} Ly6G^{+} neutrophils from non-inoculated mice (grey) or *S. aureus*-inoculated mice (blue). Data are median (±min/max) and *n* = 5. Statistical test used: an ANOVA. *$p < 0.05$ and **$p < 0.01$.

4

Figure 6, (A) Haematoxylin and eosin stains of negative control, positive control due to GM-CSF and G-CSF treatment, or *S. aureus* SAC-exposed human bone marrow cells. From the above-mentioned cultures, CD11b^low/- myeloid cells were isolated and used in

a T cell proliferation assay with PKH-stained PBMC. Absolute cell numbers of (B) CD3+ CD4+ T cells and (C) of CD3+ CD8α+ T cells were determined with flow analysis of PKH-stained PBMC mono-cultures (black) without or with anti-CD3/CD28 stimulation and from PKH-stained and anti-CD3/CD28-stimulated PBMCs co-cultured with CD11b$^{low/–}$ myeloid cells from negative control or *S. aureus* SAC co-culture samples in a 1:1 ratio (light grey). Data are mean (±SD) and are from three (positive control) or four (negative control and *S. aureus* SACs) independent experiments with three or four different human bone marrow donors, respectively. (D) Analytes measured in 3 d old culture supernatants of either negative control (black), positive control (grey), or SAC-exposed (blue) human bone marrow cell cultures present after 3 d culture. Data are median (±min/max), *n* = 3 (positive control), and *n* = 4 (negative control and *S. aureus* SACs). Statistical tests used: Holm-Sidak's multiple comparison test. #*p* ≤ 0.1, *p < 0.05, ***p < 0.001, and ****p < 0.0001.

In cell culture of 3 d cultures supernatant of the positive control bone marrow cells GM-CSF, IFNγ, and IL-12p70 were found in abundance, whereas 3 d old supernatants from SAC – bone marrow co-cultures contained elevated levels of GM-CSF, IL-6, TNFα, IL-1β, IL-12p70, IL-8, and IL-10 (Figure 6D).

DISCUSSION

MDSCs have been associated with chronic *S. aureus* infections[3,13-18] and recently it has been suggested that cells close to SACs and within abscesses in an *S. aureus* bone infection in mice might be MDSCs[3]. To investigate whether SACs cause MDSC expansion, we co-cultured human and murine bone marrow cells with our previously developed 3D *in vitro* SAC model and showed that indeed SAC-exposed human and murine bone marrow cells had immunosuppressive abilities and lowered absolute T cell numbers in a similar manner as monocytic MDSCs isolated from mice with an *S. aureus* bone infection. Furthermore, we characterized possible mediators that might be linked to MDSC expansion, activation, and immunosuppressive functioning due to SACs. This is, to the best of our knowledge, the first time that a direct link between SACs and MDSC induction has been reported.

As mentioned above, factors involved in MDSC expansion include GM-CSF, G-CSF, M-CSF, VEGF, and IL-6. These factors prevent immature myeloid cells to differentiate into mature cells by increasing STAT3 signalling[7,11,12]. Increased levels of IL-6 were detected in SAC – human and murine bone marrow cell co-cultures, which suggests that at least IL-6 could be involved in the expansion of MDSCs in these cultures. Previously, it has been shown

4

that *S. aureus* biofilm-induced MDSCs have an increased IL-6 expression compared to non-treated cells[17], being in line with this study. GM-CSF and VEGF were also present in our SAC-exposed bone marrow cultures, suggesting that these factors also possibly play a role in MDSC expansion due to SACs *in vitro*.

Furthermore, TLR activation by *S. aureus* lipoproteins can result in MDSC expansion and can regulate MDSC functioning; during an *S. aureus* skin infection, resident skin cells were stimulated to secrete IL-6 by TLR2 activation, which resulted in recruitment and accumulation of MDSCs[13], and TLRs regulate the immunosuppressive function of MDSCs by upregulation of iNOS and Arg-1 through MyD88 and NF-κB signalling[11]. In contrast, a lack of TLR activation has been reported beneficial for MDSC maintenance by suppressing maturation of the cells as well[27-29]. It is likely that TLR ligands of *S. aureus* that grow in SAC form are not easily accessible for immune cells, since that SACs are covered with a fibrin pseudocapsule which blocks access to immune cells[21], and possibly also not well released from the SAC. Therefore, the SACs might not provide or secrete the proper stimuli to activate TLRs, such as TLR9[27-29], of the bone marrow myeloid cells in order for them to mature, forcing the cells to remain immature and facilitating the maintenance of the MDSCs. In line with this hypothesis, co-culturing of dispersed, free *S. aureus* with murine bone marrow cells resulted in different monocyte and neutrophil ratio's than co-culturing with *in vitro* SACs and dispersed *S. aureus*-exposed monocytes and neutrophils had a different appearance than SAC-exposed monocytes and neutrophils.

Hypoxia is another driving factor of MDSC differentiation and functioning through hypoxia-inducible factor (HIF)-α stabilisation and transcription of HIF target genes[7,30]. The *S. aureus* SACs elaborate their fibrin network, other than the fibrin pseudocapsule, when in culture with bone marrow cells. It may be that given that the bone marrow cells are covered within this fibrin web, but possibly also because *S. aureus* is using oxygen, the growth conditions for the bone cells are more hypoxic and HIF-α stabilisation with subsequent effects occurs, resulting in MDSC expansion from the bone marrow cells. During hypoxia the cells will use glycolysis as metabolic pathway, a metabolic characteristic of MDSCs[7], and hypoxia can trigger autophagy[30]. Interestingly, presence of proteins indicating that glycolysis and autophagy (Eno2, and

Snap29 and TPP1, respectively), occurred in the SAC – bone marrow co-culture, suggest that hypoxia might be a factor of MDSC induction due to *S. aureus* SACs. Future research clarifying this is required.

Prolonged exposure to pro-inflammatory cytokines leads to the activation of MDSCs[11,12]. Indeed, in the *in vitro* SAC – human and murine bone marrow cell co-cultures elevated levels of the pro-inflammatory cytokines IL-1β and TNFα were found. Also, the cytokine IL-12p70 was found in high concentrations in SAC-exposed human bone marrow cultures. The cytokine IL-12 has been linked to MDSC recruitment in a *S. aureus* prosthetic joint infection in mice and was found to be an important factor for the anti-inflammatory, persistent environment associated with biofilm[15].

Factors that contribute to the immunosuppressive activity of MDSCs are the enzymes Arg-1 (M-MDSCs and G-MDSCs) and iNOS (M-MDSCs) and their downstream metabolites such as NO and ROS, and the cytokines IL-10 and TGF-β[8]. SAC-exposed monocytes indeed expressed Arg-1 and iNOS, and SAC-exposed neutrophils expressed Arg-1, indicating that their immunosuppressive actions might be mediated by these enzymes. Further research is required to quantify these or downstream metabolites such as NO, kynurenines, ornithine, urea and polyamines[8]. Also, IL-10 and TGF-β were present in SAC – bone marrow cultures and might also contribute to the immunosuppressive abilities of SAC-exposed monocytes and neutrophils. In line with our finding, *S. aureus* biofilm-induced MDSCs had increased expression of Arg-1, iNOS, and IL-10[14,16,17] and cells from *S. aureus*-infected mice secreted high levels of IL-10 and TGF-β compared to cells of non-infected mice, although it was argued that cell-cell proximity was more important for the immunosuppressive abilities of the *S. aureus*-exposed cells than IL-10 and TGF-β[18].

Aside from *in vitro* SACs causing MDSC expansion and activation in an indirect manner, by stimulating eukaryotic cells to secrete cytokines and growth factors, *S. aureus* might also directly induce MDSC expansion and activation. Recently, it has been reported that staphylococcal enterotoxin A and B cause G-MDSC expansion from human PBMCs, which were able to reduce T cell proliferation[31]. Furthermore, *S. aureus* biofilm that was unable to secrete D- and L-lactate lowered the secretion of IL-10 by MDSCs[32], and the synovial fluid of patients with prosthetic joint infection, known to have

4

MDSC-like cells[33], had elevated levels of lactate[32]. Investigations into whether these above-mentioned *S. aureus* proteins among others are involved in MDSC expansion due to *in vitro* and *in vivo* SACs have yet to be performed and are subject of current experiments.

It appears that *in vitro* SACs triggered similar expansion and activation mechanisms in murine and in human bone marrow cells. However, the immunosuppression of CD4^{+} and CD8α^{+} T cells by the SAC-exposed human CD11b^{low/−} myeloid cells was mainly through lowering their absolute numbers, whereas SAC-exposed murine CD11b^{+} Gr-1^{+} also decreased proliferation rates of CD4^{+} T cells. Similarities between the *in vitro* and *ex vivo* cultures were the detected proteins HGF, PDGFB, IL-10, TGF-β, IL-17A. The proteins HGF and PDGFB are both involved in fibrosis[34] which is especially interesting given that fibrosis is required for encapsulating the SAC and the immune cells around SAC to form an abscess. Whether MDSCs might facilitate fibrosis and, subsequently, also in this manner help *S. aureus* within SACs to persist is important to investigate in future.

In this study, the effect of SAC-exposed bone marrow monocytes and neutrophils on CD4^{+} and CD8α^{+} T cells was investigated. However, it is known from the cancer field that the tumor microenvironment, which MDSCs are part of, is immune cell rich and that other cells such as M2 macrophages, dendritic cells, and Tregs also facilitate the immunosuppressive milieu[10,35]. It would be interesting to examine the influence of SAC-induced MDSCs on these cell types as well. Tregs and macrophages would especially be interesting candidates; both are induced by MDSCs through IL-10 and TGF-β[10,36], and these cytokines were present in SAC – bone marrow co-cultures. Also, MDSCs can suppress B cells, NK cells, dendritic cells, and macrophages[10,37], and little is known on how these cells are impacted by *S. aureus* (SAC)-induced MDSCs. This might also be studied in future with the experimental set-up used in the present study. MDSCs, as part of the tumor microenvironment, not only affect immune cells, but also stromal cells[38,39]. It would be interesting to clarify whether SAC-induced MDSCs also have this activity.

Besides the similarities of a tumor microenvironment and *S. aureus* abscesses, there are important differences. In *S. aureus* abscesses there is a viable core, the fibrin-encapsulated SAC[3], whereas in a tumor there is

a necrotic core due to poor diffusion of oxygen and nutrients throughout the tumor[10,40,41]. The SAC's fibrin pseudocapsule acts as a physical barrier for the immune cells[21], which is something that immune cells within a tumor do not encounter[40]. Furthermore, *S. aureus* within SAC structures may secrete a variety of virulence factors such as staphylococcal enterotoxins[42], staphylococcal protein A (SpA)[43,44], and pore-forming toxins[45] that actively and directly target not only innate immune cells but also lymphoid cells.

We did not distinguish between M-MDSCs or G-MDSCs for the T cell proliferation assays with *in vitro* SAC-exposed bone marrow cells. It would be interesting to assess whether SAC-induced M-MDSCs and G-MDSCs possibly differ in their immunosuppressive actions as was observed for the *ex vivo* cultures with monocytes or neutrophils from *S. aureus*-infected mice.

By using an 3D *in vitro* SAC model, we have demonstrated that immunosuppressive MDSCs, which mainly lowered T cell numbers, are induced from both murine and human bone marrow cells by the presence of *S. aureus* SACs. Furthermore, mediators in the expansion, activation, and immunosuppressive activity of the SAC-induced MDSCs were identified. Inhibition of these mediators, and thus of the expansion and activities of MDSCs, could possibly prevent establishment of the immunosuppressive environment associated with chronic, persistent *S. aureus* infections and might provide an additional strategy for treating chronic *S. aureus* infections

ACKNOWLEDGMENTS

4

REFERENCES

1. Brandt, S. L., Putnam, N. E., Cassat, J. E. & Serezani, C. H. Innate Immunity to Staphylococcus aureus: Evolving Paradigms in Soft Tissue and Invasive Infections. *Journal of immunology (Baltimore, Md. : 1950)* **200**, 3871-3880, doi:10.4049/jimmunol.1701574 (2018).

2. Farnsworth, C. W. *et al.* Adaptive Upregulation of Clumping Factor A (ClfA) by Staphylococcus aureus in the Obese, Type 2 Diabetic Host Mediates Increased Virulence. *Infection and immunity* **85**, doi:10.1128/iai.01005-16 (2017).

3. Hofstee, M. I. *et al.* A murine Staphylococcus aureus fracture-related infection model characterised by fracture non-union, staphylococcal abscess communities and myeloid-derived suppressor cells. *European Cells & Materials* **41**, 774-792, doi:10.22203/eCM.v041a49 (2021).

4. Cheng, A. G. *et al.* Contribution of coagulases towards Staphylococcus aureus disease and protective immunity. *PLoS Pathog* **6**, e1001036, doi:10.1371/journal.ppat.1001036 (2010).

5. Ostrand-Rosenberg, S. & Fenselau, C. Myeloid-Derived Suppressor Cells: Immune-Suppressive Cells That Impair Antitumor Immunity and Are Sculpted by Their Environment. *Journal of immunology (Baltimore, Md. : 1950)* **200**, 422-431, doi:10.4049/jimmunol.1701019 (2018).

6. Veglia, F., Perego, M. & Gabrilovich, D. Myeloid-derived suppressor cells coming of age. *Nature immunology* **19**, 108-119, doi:10.1038/s41590-017-0022-x (2018).

7. Veglia, F., Sanseviero, E. & Gabrilovich, D. I. Myeloid-derived suppressor cells in the era of increasing myeloid cell diversity. *Nature reviews. Immunology* **21**, 485-498, doi:10.1038/s41577-020-00490-y (2021).

8. Bronte, V. *et al.* Recommendations for myeloid-derived suppressor cell nomenclature and characterization standards. *Nature Communications* **7**, 12150, doi:10.1038/ncomms12150 (2016).

9. Rodríguez, P. C. & Ochoa, A. C. Arginine regulation by myeloid derived suppressor cells and tolerance in cancer: mechanisms and therapeutic perspectives. *Immunological Reviews* **222**, 180-191, doi:10.1111/j.1600-065X.2008.00608.x (2008).

10. Groth, C. *et al.* Immunosuppression mediated by myeloid-derived suppressor cells (MDSCs) during tumour progression. *British Journal of Cancer* **120**, 16-25, doi:10.1038/s41416-018-0333-1 (2019).

11. Medina, E. & Hartl, D. Myeloid-Derived Suppressor Cells in Infection: A General Overview. *Journal of Innate Immunity* **10**, 407-413, doi:10.1159/000489830 (2018).

12. Ost, M. *et al.* Myeloid-Derived Suppressor Cells in Bacterial Infections. *Frontiers in Cellular and Infection Microbiology* **6**, 37, doi:10.3389/fcimb.2016.00037 (2016).

13. Skabytska, Y. *et al.* Cutaneous innate immune sensing of Toll-like receptor 2-6 ligands suppresses T cell immunity by inducing myeloid-derived suppressor cells. *Immunity* **41**, 762-775, doi:10.1016/j.immuni.2014.10.009 (2014).

14. Heim, C. E., Vidlak, D. & Kielian, T. Interleukin-10 production by myeloid-derived suppressor cells contributes to bacterial persistence during Staphylococcus aureus orthopedic biofilm infection. *Journal of leukocyte biology* **98**, 1003-1013, doi:10.1189/jlb.4VMA0315-125RR (2015).

15. Heim, C. E. *et al.* IL-12 promotes myeloid-derived suppressor cell recruitment and bacterial persistence during Staphylococcus aureus orthopedic implant infection. *Journal of immunology (Baltimore, Md. : 1950)* **194**, 3861-3872, doi:10.4049/jimmunol.1402689 (2015).

16. Heim, C. E. *et al.* Myeloid-derived suppressor cells contribute to Staphylococcus aureus orthopedic biofilm infection. *Journal of immunology (Baltimore, Md. : 1950)* **192**, 3778-3792, doi:10.4049/jimmunol.1303408 (2014).

17. Peng, K. T. *et al.* Staphylococcus aureus biofilm elicits the expansion, activation and polarization of myeloid-derived suppressor cells in vivo and in vitro. *PloS one* **12**, e0183271, doi:10.1371/journal.pone.0183271 (2017).

18. Tebartz, C. *et al.* A major role for myeloid-derived suppressor cells and a minor role for regulatory T cells in immunosuppression during Staphylococcus aureus infection. *Journal of immunology (Baltimore, Md. : 1950)* **194**, 1100-1111, doi:10.4049/jimmunol.1400196 (2015).

19. Masters, E. A. *et al.* Evolving concepts in bone infection: redefining "biofilm", "acute vs. chronic osteomyelitis", "the immune proteome" and "local antibiotic therapy". *Bone research* **7**, 20, doi:10.1038/s41413-019-0061-z (2019).

20. Bader, J. E., Voss, K. & Rathmell, J. C. Targeting Metabolism to Improve the Tumor Microenvironment for Cancer Immunotherapy. *Molecular Cell* **78**, 1019-1033, doi:10.1016/j.molcel.2020.05.034 (2020).

21. Hofstee, M. I. *et al.* Three-Dimensional In Vitro Staphylococcus aureus Abscess Communities Display Antibiotic Tolerance and Protection from Neutrophil Clearance. *Infection and immunity* **88**, doi:10.1128/iai.00293-20 (2020).

22. Moriarty, T. F., Campoccia, D., Nees, S. K., Boure, L. P. & Richards, R. G. In vivo evaluation of the effect of intramedullary nail microtopography on the development of local infection in rabbits. *The International journal of artificial organs* **33**, 667-675, doi:10.1177/039139881003300913 (2010).

23. Heilmann, C., Gerke, C., Perdreau-Remington, F. & Gotz, F. Characterization of Tn917 insertion mutants of Staphylococcus epidermidis affected in biofilm formation. *Infection and immunity* **64**, 277-282 (1996).

24. Solito, S. *et al.* Methods to Measure MDSC Immune Suppressive Activity In Vitro and In Vivo. *Current Protocols in Immunology* **124**, e61, doi:10.1002/cpim.61 (2019).

25. Marigo, I. *et al.* Tumor-induced tolerance and immune suppression depend on the C/EBPbeta transcription factor. *Immunity* **32**, 790-802, doi:10.1016/j.immuni.2010.05.010 (2010).

26. Solito, S. *et al.* A human promyelocytic-like population is responsible for the immune suppression mediated by myeloid-derived suppressor cells. *Blood* **118**, 2254-2265, doi:10.1182/blood-2010-12-325753 (2011).

27. Shirota, Y., Shirota, H. & Klinman, D. M. Intratumoral injection of CpG oligonucleotides induces the differentiation and reduces the immunosuppressive activity of myeloid-derived suppressor cells. *Journal of immunology (Baltimore, Md. : 1950)* **188**, 1592-1599, doi:10.4049/jimmunol.1101304 (2012).

28. Zhou, H., Jiang, M., Yuan, H., Ni, W. & Tai, G. Dual roles of myeloid-derived suppressor cells induced by Toll-like receptor signaling in cancer. *Oncology Letters* **21**, 149, doi:10.3892/ol.2020.12410 (2021).

4

29. Zoglmeier, C. *et al.* CpG blocks immunosuppression by myeloid-derived suppressor cells in tumor-bearing mice. *Clinical Cancer Research* **17**, 1765-1775, doi:10.1158/1078-0432.Ccr-10-2672 (2011).

30. Wang, B. *et al.* Targeting hypoxia in the tumor microenvironment: a potential strategy to improve cancer immunotherapy. *Journal of Experimental & Clinical Cancer Research* **40**, 24, doi:10.1186/s13046-020-01820-7 (2021).

31. Stoll, H. *et al.* Staphylococcal Enterotoxins Dose-Dependently Modulate the Generation of Myeloid-Derived Suppressor Cells. *Frontiers in Cellular and Infection Microbioly* **8**, 321, doi:10.3389/fcimb.2018.00321 (2018).

32. Heim, C. E. *et al.* Lactate production by Staphylococcus aureus biofilm inhibits HDAC11 to reprogramme the host immune response during persistent infection. *Nature Microbioly* **5**, 1271-1284, doi:10.1038/s41564-020-0756-3 (2020).

33. Heim, C. E. *et al.* Human prosthetic joint infections are associated with myeloid-derived suppressor cells (MDSCs): Implications for infection persistence. *Journal of Orthopaedic Research* **36**, 1605-1613, doi:10.1002/jor.23806 (2018).

34. Koch, P. S., Lee, K. H., Goerdt, S. & Augustin, H. G. Angiodiversity and organotypic functions of sinusoidal endothelial cells. *Angiogenesis* **24**, 289-310, doi:10.1007/s10456-021-09780-y (2021).

35. Dora, D. *et al.* Characterization of Tumor-Associated Macrophages and the Immune Microenvironment in Limited-Stage Neuroendocrine-High and -Low Small Cell Lung Cancer. *Biology* **10**, doi:10.3390/biology10060502 (2021).

36. Huang, B. *et al.* Gr-1+CD115+ immature myeloid suppressor cells mediate the development of tumor-induced T regulatory cells and T-cell anergy in tumor-bearing host. *Cancer Research* **66**, 1123-1131, doi:10.1158/0008-5472.Can-05-1299 (2006).

37. Dorhoi, A. & Du Plessis, N. Monocytic Myeloid-Derived Suppressor Cells in Chronic Infections. *Frontiers in Immunology* **8**, 1895, doi:10.3389/fimmu.2017.01895 (2017).

38. Ma, X., Wang, M., Yin, T., Zhao, Y. & Wei, X. Myeloid-Derived Suppressor Cells Promote Metastasis in Breast Cancer After the Stress of Operative Removal of the Primary Cancer. *Frontiers in Oncology* **9**, 855, doi:10.3389/fonc.2019.00855 (2019).

39. Ren, X. *et al.* Inhibition of CCL7 derived from Mo-MDSCs prevents metastatic progression from latency in colorectal cancer. *Cell death & disease* **12**, 484, doi:10.1038/s41419-021-03698-5 (2021).

40. Jin, M. Z. & Jin, W. L. The updated landscape of tumor microenvironment and drug repurposing. *Signal Transduction and Targeted Therapy* **5**, 166, doi:10.1038/s41392-020-00280-x (2020).

41. Tomes, L. *et al.* Necrosis and hypoxia in invasive breast carcinoma. *Breast Cancer Research and Treatment* **81**, 61-69, doi:10.1023/a:1025476722493 (2003).

42. Llewelyn, M. & Cohen, J. Superantigens: microbial agents that corrupt immunity. *The Lancet Infectious Diseases* **2**, 156-162, doi:10.1016/s1473-3099(02)00222-0 (2002).

43. Goodyear, C. S. & Silverman, G. J. Death by a B cell superantigen: In vivo VH-targeted apoptotic supraclonal B cell deletion by a Staphylococcal Toxin. *Journal of Experimental Medicine* **197**, 1125-1139, doi:10.1084/jem.20020552 (2003).

44. Graille, M. *et al.* Crystal structure of a Staphylococcus aureus protein A domain complexed with the Fab fragment of a human IgM antibody: structural basis for recognition of B-cell receptors and superantigen activity. *Proceedings of the National Academy of Sciences of the United States of America* **97**, 5399-5404, doi:10.1073/pnas.97.10.5399 (2000).

45. Spaan, A. N., van Strijp, J. A. G. & Torres, V. J. Leukocidins: staphylococcal bi-component pore-forming toxins find their receptors. *Nature reviews. Microbiology* **15**, 435-447, doi:10.1038/nrmicro.2017.27 (2017).

4

SUPPLEMENTARY DATA

Supplementary table 1. Protein biomarker analysis of murine positive control and SAC-exposed bone marrow cultures in comparison to negative control bone marrow cells. Significantly differently expressed proteins are in bold.

Analyte	Positive control				S. aureus SACs			
	NPX	Min	Max	p-value	NPX	Min	Max	p-value
Acvrl1	0.080198	-0.10633	0.266722	0.53909	0.506429	0.319904	0.692953	**1.51E-06**
Adam23	-0.01126	-0.33606	0.313531	0.995875	0.057263	-0.26753	0.382057	0.899103
Ahr	0.519393	0.118256	0.920531	**0.009555**	0.420159	0.019021	0.821296	**0.038837**
Apbb1ip	-0.0693	-0.34946	0.210868	0.811916	0.034648	-0.24552	0.314813	0.948893
Axin1	0.093668	-0.14632	0.333658	0.599518	0.106194	-0.1338	0.346185	0.520293
Ca13	0.188117	-0.22917	0.605408	0.507943	0.138142	-0.27915	0.555433	0.690413
Cant1	-0.0036	-0.32141	0.314206	0.999559	0.31755	-0.00026	0.635356	0.050212
Casp3	0.162021	-0.34083	0.664871	0.703805	1.607817	1.104966	2.110667	**9.60E-08**
Ccl2	8.81005	8.017551	9.602549	**2.10E-14**	9.148914	8.356415	9.941414	**2.10E-14**
Ccl20	0.026476	-0.31521	0.368161	0.979587	0.36247	0.020785	0.704155	**0.03612**
Ccl3	5.38239	4.80773	5.95705	**2.11E-14**	9.413543	8.838884	9.988203	**2.10E-14**
Ccl5	-0.05182	-0.40103	0.297393	0.927331	2.184746	1.835534	2.533957	**1.55E-13**
Cdh6	-0.00492	-0.1965	0.186668	0.997737	0.049103	-0.14248	0.240689	0.799667
Clmp	0.10242	-0.24738	0.452218	0.747615	0.04704	-0.30276	0.396838	0.93988
Clstn2	0.083914	-0.26573	0.433555	0.821784	0.205938	-0.1437	0.555578	0.322245
Cntn1	-0.00673	-0.52663	0.513157	0.999423	2.099522	1.579631	2.619413	**1.23E-09**
Cntn4	-0.0538	-0.58783	0.480234	0.965765	2.014092	1.480063	2.548122	**4.61E-09**
Cpe	0.117222	-0.12702	0.361461	0.465457	0.124439	-0.1198	0.368677	0.423963
Crim1	0.904332	0.541812	1.266853	**5.66E-06**	1.319222	0.956702	1.681743	**9.08E-09**
Csf2	12.41882	11.65896	13.17868	**2.10E-14**	1.680909	0.921049	2.440769	**3.21E-05**
Cxcl1	0.495879	-0.38927	1.381028	0.357239	8.059759	7.17461	8.944908	**2.11E-14**

Cxcl9	0.161654	-0.36769	0.690995	0.72902	0.587522	0.058182	1.116863	**0.027592**
Cyr61	0.174816	-0.178844	0.528071	0.444285	0.385834	0.032579	0.73909	0.051
Dctn2	-0.14064	-0.49816	0.216891	0.59482	0.088564	-0.26896	0.446092	0.811418
Ddah1	0.2086	-0.04211	0.459306	0.115792	0.668212	0.417506	0.918918	**2.03E-06**
Dlk1	0.025326	-0.56809	0.618744	0.993759	2.261857	1.668439	2.855275	**3.77E-09**
Dll1	-0.05614	-0.44964	0.337354	0.93261	1.280693	0.887197	1.67419	**7.01E-08**
Eda2r	0.134764	-0.05114	0.320672	0.187645	0.163271	-0.02264	0.349179	0.092779
Eno2	0.102199	-0.16202	0.36642	0.604902	0.312828	0.048607	0.577049	**0.018189**
Epcam	0.086451	-0.4128	0.585706	0.902476	2.609799	2.110544	3.109054	**6.37E-12**
Epo	0.031233	-0.12164	0.184105	0.867108	0.054049	-0.09882	0.20692	0.656011
Erbb4	-0.06824	-0.33292	0.196436	0.79755	0.285387	0.020708	0.550065	**0.032852**
Fas	0.61854	0.093644	1.143436	**0.018774**	0.806113	0.281217	1.33101	**0.002221**
Fli1	-0.00022	-0.29004	0.289609	0.999998	0.151759	-0.13807	0.441583	0.404773
Flrt2	0.05412	-0.37678	0.485023	0.9947334	0.131029	-0.29987	0.561932	0.730964
Foxo1	-0.00503	-0.27401	0.263956	0.998801	0.09932	-0.16966	0.368301	0.631898
Fst	0.815567	0.438595	1.192539	**4.34E-05**	0.587228	0.210256	0.9642	**0.001938**
Fstl3	-0.02648	-0.2431	0.190139	0.950036	0.579132	0.362515	0.79575	**1.93E-06**
Gcg	0.03534	-0.2574	0.328082	0.951235	0.016187	-0.27656	0.308929	0.989548
Gdnf	0.170066	-0.13813	0.478262	0.367873	0.108646	-0.19955	0.416842	0.657604
Gfra1	-0.02679	-0.31688	0.263294	0.97113	0.413452	0.123364	0.703541	**0.004371**
Ghrl	0.0107	-0.23806	0.259458	0.99366	0.164297	-0.08446	0.413054	0.245085
Hgf	0.196818	-0.08861	0.482241	0.21774	0.365352	0.079929	0.650776	**0.010423**
Igsf3	-0.06644	-0.33758	0.204706	0.815058	-0.02151	-0.29266	0.249628	0.978608
Il10	-0.06541	-0.49268	0.36185	0.922842	2.157867	1.730602	2.585131	**1.32E-11**
Il17a	-0.01264	-0.39992	0.374638	0.996344	0.573626	0.186346	0.960905	**0.003108**
Il17f	-0.02632	-0.27593	0.223292	0.962557	0.20612	-0.04349	0.455732	0.119267
Il1a	4.194051	3.4792	4.908902	**5.53E-13**	4.300574	3.585724	5.015425	**3.31E-13**
Il1b	0.065698	-0.25462	0.386018	0.866158	0.443	0.122679	0.763321	**0.005646**

4

Il23r	-0.04612	-0.36224	0.270005	0.929666	0.142314	-0.17381	0.458436	0.508855
Il5	-0.15824	-0.4759	0.159417	0.439694	-0.14442	-0.46208	0.173235	0.502263
Il6	4.927272	3.871304	5.98324	**6.80E-11**	1.640776	0.584807	2.696744	**0.001986**
Itgb1bp2	0.076324	-0.19914	0.35179	0.770417	0.01815	-0.25732	0.293617	0.985192
Itgb6	-0.13787	-0.44078	0.165038	0.501518	0.082794	-0.22011	0.385701	0.775762
Kitlg	0.014881	-0.3258	0.355562	0.993463	0.816732	0.476052	1.157413	**1.02E-05**
Lgmn	0.353468	0.177983	0.528953	**0.000111**	0.309749	0.134264	0.485234	**0.000531**
Lpl	1.049864	0.825866	1.273862	**6.20E-11**	0.209558	-0.01444	0.433556	0.069765
Map2k6	0.133862	-0.06013	0.327856	0.217319	-0.02418	-0.21818	0.169811	0.948094
Matn2	0.221934	-0.29886	0.74273	0.544843	2.661233	2.140438	3.182029	**1.03E-11**
Mia	-0.19875	-0.70371	0.306221	0.594476	0.504191	-0.00078	1.009159	0.050406
Nadk	0.147844	-0.42201	0.717694	0.79531	0.851318	0.281468	1.421168	**0.002873**
Notch3	0.089583	-0.24539	0.424555	0.784122	0.826023	0.491052	1.160995	**6.73E-06**
Ntf3	0.025131	-0.2445	0.294765	0.970612	0.155987	-0.11365	0.425621	0.334743
Pak4	0.092524	-0.20802	0.393066	0.72534	0.336746	0.036204	0.637287	**0.026021**
Parp1	-0.58837	-1.09156	-0.08519	**0.019772**	0.047144	-0.45604	0.550328	0.970309
Pdgfb	0.037697	-0.15819	0.233584	0.881089	0.525714	0.329827	0.721602	**1.82E-06**
Pla2g4a	0.348788	-0.00185	0.699426	0.051406	0.155657	-0.19498	0.506295	0.518162
Plin1	0.34824	0.068069	0.628411	**0.012947**	0.224896	-0.05528	0.505066	0.132754
Plxna4	0.008657	-0.34264	0.359954	0.997915	0.210167	-0.14113	0.561464	0.311453
Ppp1r2	0.165978	-0.27827	0.610226	0.625172	0.334666	-0.10958	0.778913	0.165831
Prdx5	-2.78212	-4.5173	-1.04694	**0.00146**	-1.60032	-3.3351	0.134857	0.074592
Qdpr	0.04046	-0.23112	0.312042	0.926772	0.15402	-0.11756	0.425602	0.348649
Rgma	-0.09465	-0.57274	0.383433	0.874636	1.706359	1.228274	2.184444	**1.30E-08**
Riox2	1.541017	1.083306	1.998727	**3.81E-08**	0.397518	-0.06019	0.855228	0.097281
S100a4	0.341681	-0.15354	0.836906	0.217391	-0.15743	-0.65265	0.337795	0.710301
Sez6l2	0.032767	-0.12533	0.190868	0.863556	0.055233	-0.10287	0.213335	0.66246

Snap29	1.545736	1.041776	2.049695	**1.98E-07**	0.750219	0.246259	1.254178	**0.002968**
Tgfa	0.196557	0.042878	0.350235	**0.010486**	0.12057	-0.03311	0.274249	0.144228
Tgfb1	0.188951	-0.03432	0.412218	0.108228	0.50146	0.278194	0.724726	**2.60E-05**
Tgfbr3	-0.05662	-0.60453	0.491283	0.964004	3.022201	2.474295	3.570107	**2.03E-12**
Tnf	0.58382	0.203859	0.963781	**0.00221**	3.800423	3.420462	4.180385	**2.10E-14**
Tnfrsf11b	-0.02754	-0.37662	0.321545	0.978854	0.788291	0.439211	1.137371	**2.41E-05**
Tnfrsf12a	-0.01848	-0.28914	0.252186	0.984115	0.029839	-0.24082	0.300502	0.959149
Tnfsf12	0.232146	-0.16932	0.633615	0.335071	1.004083	0.602614	1.405552	**5.44E-06**
Tnni3	0.40275	-0.14408	0.949576	0.178473	0.30913	-0.2377	0.855956	0.350884
Tnr	0.053999	-0.21613	0.324123	0.872368	0.142816	-0.12731	0.41294	0.397983
Tpp1	0.102314	-0.25834	0.462969	0.760883	1.05846	0.697806	1.419114	**4.21E-07**
Vegfd	-0.12666	-0.43677	0.183461	0.571776	0.5082	0.198084	0.818316	**0.001171**
Vsig2	0.837719	0.557565	1.117873	**3.83E-07**	0.434447	0.211657	0.755236	**0.000513**
Wfikkn2	0.156774	-0.08696	0.400506	0.2624	0.463532	0.219801	0.707263	**0.000224**
Wisp1	-0.0803	-0.44002	0.279424	0.843672	0.229236	-0.13049	0.588957	0.268587
Yes1	-0.06831	-0.37288	0.236261	0.842321	0.003289	-0.30128	0.307858	0.999599

4